ATLAS Internal Note
PHYS-N0-076
24 November 1995

Physics Performance For Various Muon System Configurations

L. Poggioli, D. Froidevaux
CERN, Geneva, Switzerland

and

C. Guyot
Saclay, DAPNIA/SPP

Abstract

Mass resolutions and acceptances for various physics channels involving muons in the final state are studied, using a detailed parametrization of the response of the muon spectrometer for different systems, i.e. full air-core, descoped scenarios with iron end-caps or B-field reduction, and staged end-cap scenario. The impact on the ATLAS physics performance when combining the muon information with the tracker and the electron signature, if any, is also investigated.

1 Inputs

1.1 Stand-alone Muon resolution

Improved parametrized muon momentum resolutions with respect to the TP, derived from [1], have been used in this note. They provide the p_T resolutions as a function of azimuth ϕ and pseudorapidity η, for a full air-core magnet system, and for a system with air-core in the barrel and iron-core in the end-caps (4.6 m or 2 m long toroids). They take into account the $\int Bdl$ variations with the azimuth, the regions where particles see a large amount of material (coils, barrel cryostat, voussoirs), and the regions where the measurement is limited to two superlayers (coil ribs, feet, rails).

Fig. 1 (resp. Fig. 2) shows the p_T resolution versus η, for various p_T and for $\phi = 11.25^0$ (resp. $\phi = 0^0$) , for the full air-core system, where ϕ is measured with respect to a coil. These distributions have been obtained for the new reference field, equal to 85% of the nominal field studied for the TP. Fig. 3 shows the momentum resolution at $\phi = 11.25^0$ for a system with air-core in the barrel and with 4.6 m long iron-core end-caps. In this parametrization, the effect of muons showering in the iron is not taken into account in the estimated resolution, nor is the perturbation of the field in the air due to the vicinity of the iron.

1.2 Energy loss

Assuming that the average energy loss of muons in the calorimeter system can be accurately corrected for, using procedures such as GEANE, the energy loss fluctuations nevertheless dominate the momentum resolution for $p < 30$ GeV. The evaluation of the Gaussian part of these fluctuations has been parametrized using 2 Gaussians of different widths [1], and is shown in Fig. 4 (dotted curve). The tile calorimeter can provide valuable information on the energy loss fluctuations on an event by event basis. Simulations, substantiated by test beam results, predict the muon dE/dx fluctuations in the ATLAS calorimeter, based on the energy measured in the tiles [2].

Fig. 4 displays this prediction for the case where the full tile calorimeter (8.9 λ) contributes to the dE/dx measurement (dashed curve), and the case where only 67% of the calorimeter is sampled by the scintillator. This corresponds roughly to the ATLAS situation, where the tile girder and the electromagnetic calorimeter were assumed not to contribute to the energy loss measurement.
In the interesting region, i.e. $p \leq 50$ GeV, where dE/dx fluctuations in the calorimeter are a significant term in the muon momentum measurement error, the improvement from the tile measurement is rather small.

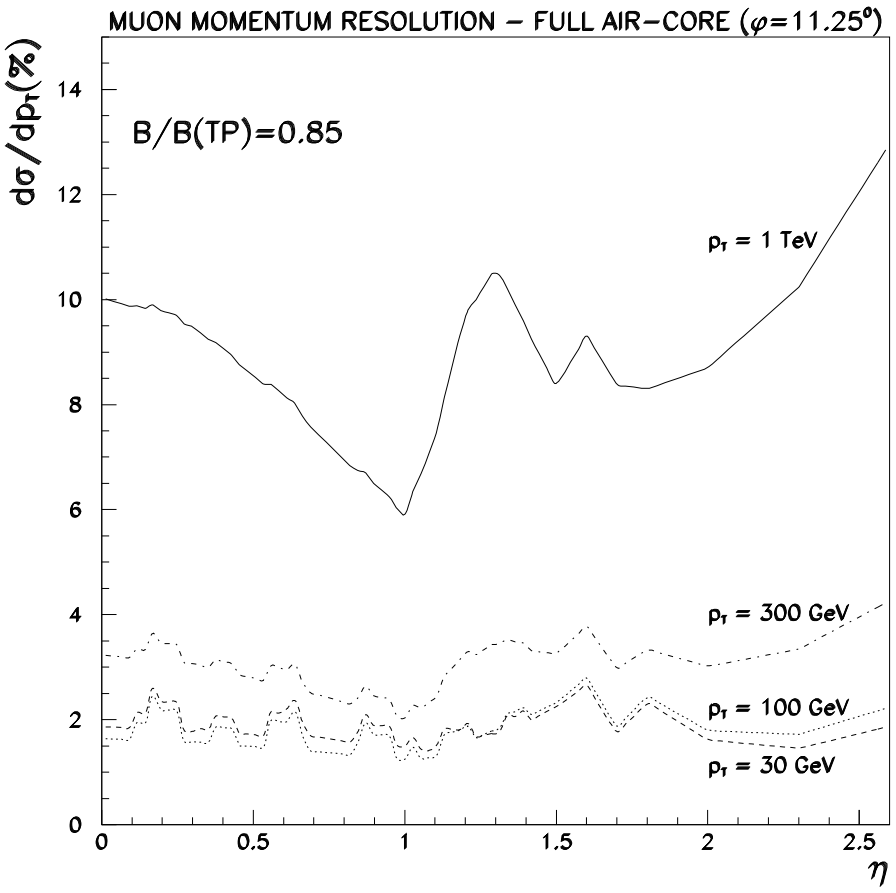

Figure 1: *p_T-resolution versus η for the full air-core system, for $\phi = 11.25^0$ with respect to a coil, and for p_T=30, 100, 300 and 1000 GeV.*

1.3 Tracker measurement

The tracker momentum resolution can be parametrized as

$$dp_T/p_T = 0.0005 \times p_T \oplus 0.012$$

over most of the η-range, except for $|\eta| \geq 2$ where the resolution degrades, as shown in Fig. 5 for the "Morges" layout (full curve) and a "descoped" layout with shorter cavity and coil (dotted curve).

For $H \rightarrow ZZ^* \rightarrow 4\mu$ decays with $m_H = 130$ GeV, the predicted 4-muon mass resolution, using the tracker alone, is 1.86 ± 0.05 GeV for the "Morges" layout. This value is in good agreement with the results obtained with full simulation and reconstruction for the TP, and the tracker momentum resolution parametrization of Fig. 5 for the "Morges" layout will therefore be used throughout the rest of

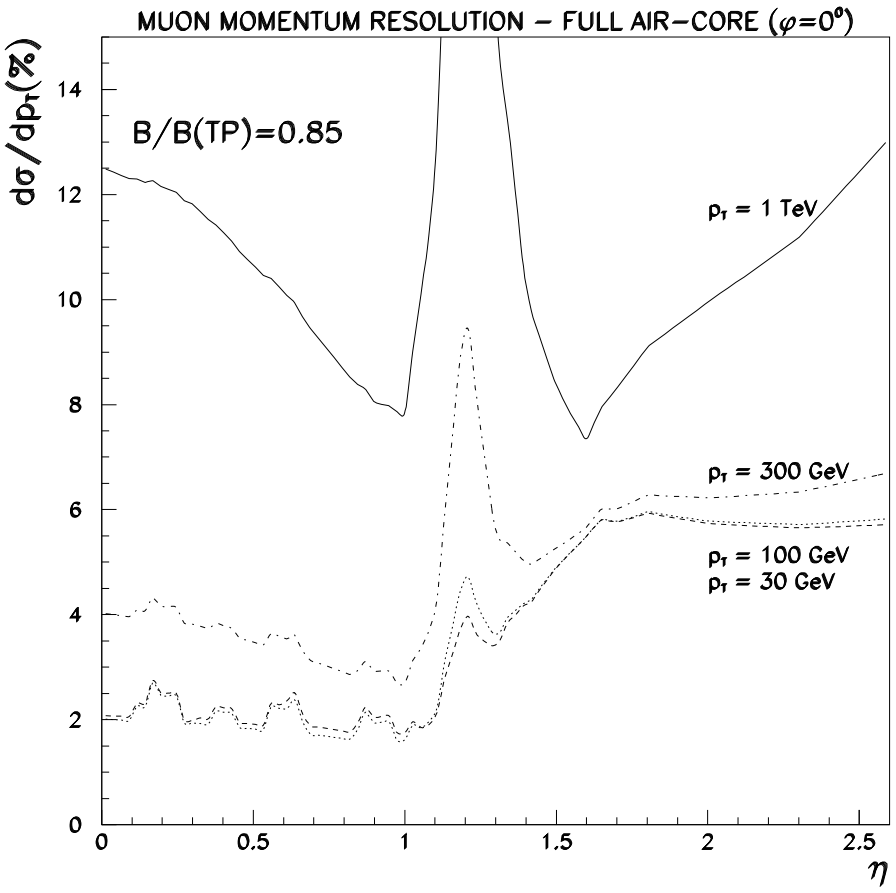

Figure 2: *Same as Fig. 1, for* $\phi = 0^0$.

this note.
A flat η-dependence of the tracker momentum resolution would only marginally improve the mass resolution quoted above. The shorter cavity scenario would result in a 6% degradation of the mass resolution.

The Higgs mass resolution has been also investigated by combining the muon and tracker information. The combined measurement of the muon 4-momentum, p_{final}, has been evaluated as :

$$p_{final} = \frac{1}{w}(p_{muon}/\sigma^2_{muon} + p_{track}/\sigma^2_{track})$$

with $w = 1/\sigma^2_{muon} + 1/\sigma^2_{track}$. The accuracies for the muon system (σ_{muon}) and for the tracker (σ_{track}) have been calculated using the parametrized expressions discussed above.

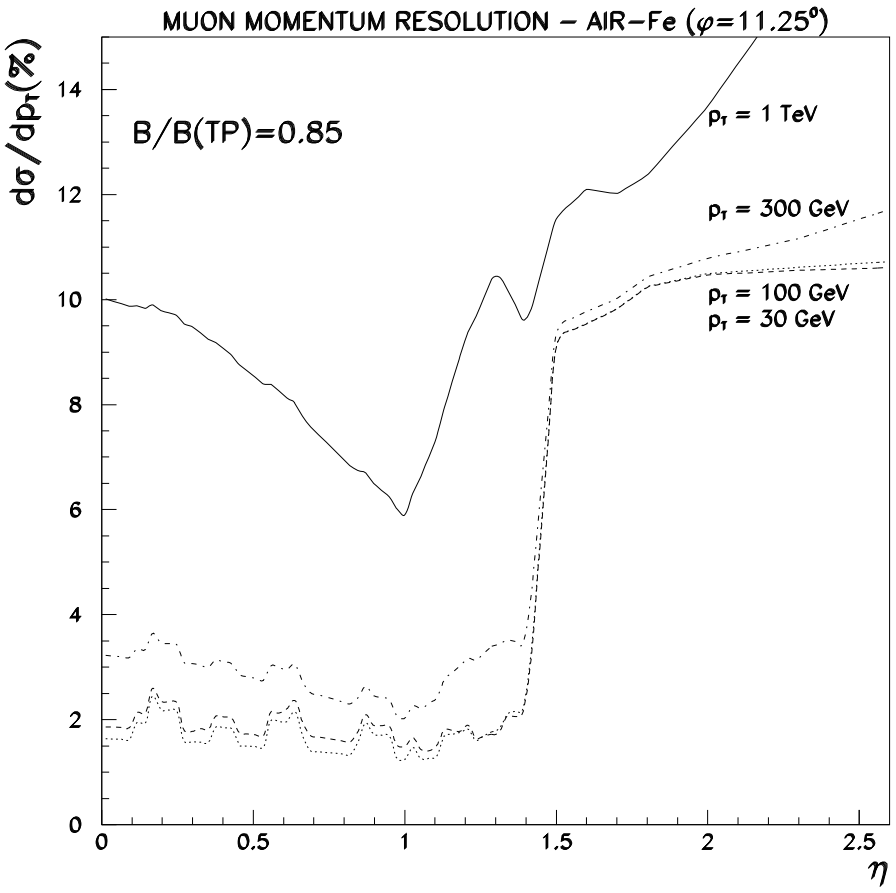

Figure 3: *p_T-resolution versus η for the air-core with 4.6 m long iron-core system, for $\phi = 11.25^0$.*

2 $H \rightarrow 4\mu$, $m_H = 130$ GeV

2.1 Introduction

For this case, and also for $m_H = 200$ GeV (see Section 3), we have used the following standard Technical Proposal selection criteria :

- Two muons with $p_T > 20$ GeV and $|\eta| < 2.5$.
- Two additional muons with $p_T > 7$ GeV and $|\eta| < 2.5$.
- One pair (1,2) of muons of appropriate charge with $m_{12} = m_Z \pm 6$ GeV.
- The other pair (3,4) of muons of appropriate charge with $m_{34} > 20$ GeV.

The limitation of the η-acceptance to 2.5 relies on the ability to reject the reducible backgrounds, namely $t\bar{t}$ and $Zb\bar{b}$. This rejection relies on :
• isolation, performed using the calorimeter and/or the tracker information, which yields a rejection of 50 for ϵ_{Higgs}=85% (resp. 50%) at low (resp. high) luminosity.
• vertexing using the tracker information, which yields an extra rejection around 10 for ϵ_{Higgs}=85% at low luminosity (i.e. for a tracker with an operational B-layer).
As it is shown in Fig. 6, increasing the acceptance from $|\eta| \geq 2.5$ to $|\eta| \geq 3$ will provide a gain in statistical significance of 5 to 10% at maximum, in the too optimistic case where the remaining background is the irreducible ZZ^*/γ^* continuum.
This brings us to a somewhat arbitrary, but at least understandable definition of muon measurements in the following :
• "stand-alone" muon measurements correspond to those where the tracker is not used, neither to improve the mass resolution nor to reject the reducible backgrounds using vertexing. It is optimistically assumed here that the geometrical acceptance of the muon system is 100% for $|\eta| < 2.5$.
• "combined" muon measurements correspond to those where the tracker is used, both for the mass resolution and for the background rejection.

As a reminder, the calorimeter mass resolution for the 4-electron channel has been evaluated with full simulation and is 1.5 GeV (resp. 1.7 GeV) at low (resp. high) luminosity, for $H \rightarrow ZZ^* \rightarrow 4e$, with $m_H = 130$ GeV.

2.2 Calculation of significances

In the following, to compare the signal significances for different systems, a Poisson estimator, given the low statistics expected in this channel, has been used instead of the Gaussian $S/\sqrt{B}$ estimator used throughout the TP. The total number of expected (S+B) events has been somewhat conservatively rounded down to the closest integer. A loss of 10% in the signal acceptance due to inner bremsstrahlung effects [3] has also been included, both for the 4-muon and the 4-electron channels.
In the cases where no tracker information is used ("stand-alone" measurement), the contribution of the $t\bar{t}$ (resp. $Zb\bar{b}$) background is increased by a factor 10 (resp. 5), since no rejection using vertexing is available. The 85% efficiency of these vertexing cuts, applied normally to the signal and the irreducible ZZ^* continuum, has been removed in such cases.
The non-Gaussian tails and the losses in acceptance have been properly taken into account. Effects from non-Gaussian tails in the mass resolution, which appear mostly in the case of "stand-alone" measurements with a mixed system (iron end-caps), and also from the corresponding loss of acceptance due to the requirement, $m_{12} = m_Z \pm 6$ GeV, quoted above, have also been properly taken into account.

2.3 Descoping

For a full air-core system, the mass resolution is found to be 1.6 $\pm$ 0.04 GeV, after applying the standard analysis cuts. This value would decrease to 1.45 GeV for the nominal TP field. The mass resolution does not scale linearly with the value of the B-field (10% loss in mass resolution for a 15% decrease of the field) since at $p_T \simeq 30$ GeV, there is still a sizeable contribution from the energy loss fluctuations. This mass resolution has to be compared to the value of 2 GeV obtained with full simulation for the TP. Part of the difference is due to a rather crude treatment of the average energy loss correction in the full simulation (it was taken to be only η-dependent), another part, to the purely Gaussian treatment of the dE/dx fluctuations in the parametrization. The mass resolutions quoted here may be therefore somewhat optimistic.

The improvement in the mass resolution using the hadron tile calorimeter measurement is small. The mass resolution improves from 1.6 $\pm$ 0.04 GeV (for 85% TP field) to 1.55 $\pm$ 0.04 GeV if one uses optimistically the tile information. If the tile calorimeter measurement is used in a more realistic way (see section 1.2) then the mass resolution is only marginally improved (1.58 $\pm$ 0.04 GeV). In the ideal case of a perfect correction (event by event) for energy loss fluctuations, the mass resolution would improve to 1.4 GeV.

The Gaussian part of the mass resolution degrades from 1.6 to 2.0 GeV for the air/iron system (Fig. 7), with non-Gaussian tails in the mass distribution from muons measured in the iron end-caps (see Table 1 for a breakdown as a function of the number of muons measured in the end-cap system).

The fraction of events which fall within $\pm 2\sigma_m$ of the Higgs mass decreases from 95% for the full air-core to 85% for the air/iron system. Moreover, the fraction of events passing the kinematic cuts is 10% lower for the air/iron system. This loss arises from the cut $m_{12} = m_Z \pm 6$ GeV (see Fig. 8).

# μ's in EC	Fraction (%)	σ_m (GeV)
0	45	1.6 $\pm$ 0.05
1	28	2.9 $\pm$ 0.2
2	16	4.2 $\pm$ 0.5
3	9	no stat.
4	2	no stat.

Table 1: *For $m_H = 130$ GeV and a system with 4.6 m long iron-core end-caps, fractions of events with various numbers of muons in the end-caps, and corresponding mass resolutions.*

For the full air-core system, the combined mass resolution (muon system and

inner detector) amounts to 1.11 GeV, whereas for the air/iron system, the combined resolution is found to be 1.27 GeV (Fig. 9). Both combined mass distributions have very small non-Gaussian tails. All these numbers are displayed in Fig. 10, as a function of the toroid B-field.

It is also important to evaluate the variations in the signal significance for various configurations, stand-alone or combined, and including the electron final states ($2e2\mu$ and 4e), which represent 75% of the statistics. The best estimates of the signal significances and the main ingredients entering the calculations are given in Table 2 (low luminosity) and Table 3 (high luminosity) for the various configurations of the muon magnet system studied here.

m_H = 130 GeV	4 μ stand-alone	4 μ combined	4 leptons(e+μ)
Air-Air B=1.00 σ_m (GeV)	1.45	1.1	1.3
Signal (events)	3.3	2.8	11.25
Background (events)	1.2	0.5	2.4
Stat. Signif. (σ)	1.8	2.2	4.6
Air-Air B=0.85 σ_m (GeV)	1.6	1.1	1.3
Signal (events)	3.3	2.8	11.25
Background (events)	1.3	0.5	2.4
Stat. Signif. (σ)	1.7	2.2	4.6
Air-Air B=0.70 σ_m (GeV)	1.8	1.2	1.35
Signal (events)	3.3	2.8	11.25
Background (events)	1.5	0.6	2.5
Stat. Signif. (σ)	1.5	2.1	4.5
Air-Iron 4.6m B=0.85 σ_m (GeV)	2.0	1.3	1.4
Signal (events)	2.7	2.7	11.0
Background (events)	1.5	0.6	2.6
Stat. Signif. (σ)	1.5	2.0	4.5

Table 2: *For $H \rightarrow ZZ^* \rightarrow$ 4-lepton decays with m_H = 130 GeV and for an integrated luminosity of 3×10^4 pb^{-1}, mass resolutions and signal significances expected from the full air-core muon system with the full TP field, with a field of 85% of the TP value, for a descoped air-core muon system with a field of 70% of the TP value, and for a descoped system with 4.6 m long iron-core end-caps. Also shown are values of the expected mass resolutions when combining the muon measurement with that of the inner detector, and when combining together all the 4-lepton final states. The muon stand-alone performance corresponds to the case where no tracker information is used (see Section 2.1).*

We recall that in this channel the full use of the tracker information is crucial to bring the reducible backgrounds ($t\bar{t}$ and $Zb\bar{b}$) well below the ZZ^*/γ^* continuum. Without this extra rejection the reducible backgrounds are at the same level as

m_H = 130 GeV	4 μ stand-alone	4 μ combined	4 leptons(e+μ)
Air-Air B=1.00 σ_m (GeV)	1.45	1.1	1.4
Signal (events)	6.5	5.5	22.0
Background (events)	2.6	1.25	6.4
Stat. Signif. (σ)	2.9	2.9	6.2
Air-Air B=0.85 σ_m (GeV)	1.6	1.1	1.4
Signal (events)	6.5	5.5	22.0
Background (events)	2.9	1.25	6.4
Stat. Signif. (σ)	2.7	2.9	6.2
Air-Air B=0.70 σ_m (GeV)	1.8	1.2	1.45
Signal (events)	6.5	5.5	22.0
Background (events)	3.3	1.4	6.6
Stat. Signif. (σ)	2.5	2.8	6.1
Air-Iron 4.6m B=0.85 σ_m (GeV)	2.0	1.3	1.5
Signal (events)	5.2	5.3	21.6
Background (events)	3.3	1.4	6.8
Stat. Signif. (σ)	2.1	2.7	6.0

Table 3: *Same as Table 2, for an integrated luminosity of* $1 \times 10^5\ pb^{-1}$. *Signal efficiencies (isolation cuts) are 40% lower than at low luminosity, due to pile-up in the calorimeter and tracker.*

the continuum, and, since they suffer from large uncertainties in their predicted rates, their contribution may well dominate the overall background.
Moreover, the signal yield is quite small in the 4-muon mode alone. This conclusion is also valid at other Higgs masses. In the most favourable case, i.e. m_H= 150 GeV, the signal yield is 18 events for one year at high luminosity, corresponding to a statistical significance of 5.4σ for "stand-alone" measurements with the baseline muon system (i.e. full air-core with 85% of the toroid B-field). The combined 4-lepton mode would in contrast allow a discovery after only one year at low luminosity (statistical significance of 5.6σ).

These two statements show that, to observe the Higgs signal in the intermediate mass range, one does need the full use of the ATLAS detector, by combining muons and electrons, and exploiting the information of the tracker. In this more realistic case, the differences in sensitivity to the signal between the various systems are quite small.

2.4 Staging

The impact on the performance of temporarily using in the end-cap region 2 m long iron-core toroids has also been investigated. As expected, the stand-alone momentum resolution deteriorates by a factor $\sqrt{2.3}$ in the end-caps with respect

to the 4.6 m long iron-core system (see Fig. 11). The momentum resolution shown in Fig.11 for the 2 meter long iron-core end-caps is obtained by performing a point-angle measurement with the full chamber system installed.

Table 4 displays, for an integrated luminosity of 3×10^{4} pb^{-1}, and for this system compared to the reference full air-core system, the expected signal and background rates and statistical significances.
The conclusions are very similar to the ones obtained in the descoping scenario. Here again, the full use of the ATLAS detector is necessary to discover the signal and in this case, only small differences with respect to the reference scenario are observed.

As studied previously [4, 5], applying a Z-mass constraint can help in the case where the Z mass resolution is significantly worse than the natural Z width.
This is only the case for the systems with iron-core end-caps (staged or descoped), and would make the potential difference between the various options even smaller.

m_H = 130 GeV	4 μ stand-alone	4 μ combined	4 leptons(e+μ)
Air-Air B=0.85 σ_m (GeV)	1.6	1.1	1.3
Signal (events)	3.3	2.8	11.25
Background (events)	1.3	0.5	2.4
Stat. Signif. (σ)	1.7	2.2	4.6
Air-Iron 2m B=0.85 σ_m (GeV)	2.1	1.3	1.4
Signal (events)	2.4	2.7	11.0
Background (events)	1.4	0.6	2.6
Stat. Signif. (σ)	1.0	2.0	4.5

Table 4: *For $H \rightarrow ZZ^{*} \rightarrow$ 4-lepton decays with m_H = 130 GeV and for an integrated luminosity of 3×10^{4} pb^{-1}, mass resolutions and signal significances expected from the full air-core muon system with a field of 85% of the TP value, and for a staged system with 2 m long iron-core end-caps. Also shown are values of the expected mass resolutions when combining the muon measurement with that of the inner detector, and when combining together all the 4-lepton final states. The muon stand-alone performance corresponds to the case where no tracker information is used (see Section 2.1).*

Finally, the effect of the global staging scenario of the ATLAS detector on the discovery potential of the intermediate mass Higgs has also been evaluated.
Apart from staging the end-cap toroids, this scenario may imply the limitation of the rapidity coverage of the precision tracker to $|\eta| < 2$ and a reduced granularity in the electromagnetic calorimeter [6]. This last point has been shown to slightly degrade the calorimeter isolation (loss of 10% in rejection), which can

nevertheless be recovered by using tracking isolation.
Most critical would be the limitation of the rapidity coverage of the central tracker. In such a case, the 4-lepton search was assumed conservatively to be limited to $|\eta| < 2$. According to Fig. 6, the loss of acceptance would be 25% for the signal and 30% for the ZZ^*/γ^* continuum, in the worst case, i.e. for m_H= 130 GeV. After correction of the signal and background rates of Table 4 for these losses, the statistical significance for observing a Higgs boson signal in this channel decreases from 4.5 to 4.1 for an integrated luminosity of 3×10^4 pb^{-1}.

3 $H \rightarrow 4\mu$, $m_H \geq 200$ GeV

In the case of a heavier Higgs, for example for $m_H = 200$ GeV with $\Gamma_H^{SM} = 1.4$ GeV, a good mass resolution may help to disentangle a SM Higgs scenario from an MSSM Higgs scenario. The same selection criteria as for $m_H = 130$ GeV were used. Table 5 summarizes the mass resolutions and the fractions of events within the nominal mass $\pm 2\sigma$, as expected for the various configurations for the 4-muon channel. The mass resolution obtained with full simulation for the 4-electron mode is 2.9 GeV at low luminosity.

$H \rightarrow ZZ \rightarrow 4\mu$	Stand-alone		Combined	
$m_H = 200$ GeV	σ_m (GeV)	# in $\pm 2\sigma_m$ (%)	σ_m (GeV)	# in $\pm 2\sigma_m$ (%)
Air-Air B=0.85	2.6	88	2.3	90
Air-Air B=0.70	3.0	88	2.6	91
Air-Fe B=0.85	3.5	78	2.6	88
Air-Fe staged	3.5	68	2.6	87

Table 5: *For $H \rightarrow ZZ \rightarrow 4\mu$ decays with $m_H = 200$ GeV and for various configurations of the muon system, mass resolutions and acceptances in mass bin. The results are shown for both the stand-alone (left) and combined (right) measurements.*

The mass resolution is directly proportional to the field intensity. In this case of a heavier Higgs boson, tails appear in the stand-alone mass distribution even for the full air-core system, as shown in Fig. 12. These tails arise from measurements with only two superlayers and from measurements in low B-field regions. In comparison to the lighter Higgs, the use of iron in the end-caps induces even more tails in the mass distribution for the stand-alone measurement (Fig. 12). In fact, the fraction of events within $\pm 2\sigma_m$ of the Higgs mass decreases from 88% for the full air-core system to 78% for the air/iron system, and to 68% for the staged iron-core end-cap system.

In this Higgs mass region, the tracker is not crucial to reject the backgrounds, since the dominant one is the ZZ continuum. The tracker still gives an impor-

tant contribution to the mass measurement, which results in an overall Gaussian response even with iron-core end-caps, as shown in Fig. 13. The fraction of events within $\pm 2\sigma_m$ of the Higgs mass increases to 88%, for all systems.
In the case of the combined measurement, the 4-muon mass resolution is 10% worse for iron-core end-caps than for the full air-core system, as shown in (Fig. 13).

As mentioned in the previous section, the use of the Z-mass constraint may slightly improve the Higgs mass resolution, thus reducing the difference between the various options. Moreover, the signal to background ratio and the overall signal rates in this channel are much larger than for m_H=130 GeV [7]. We conclude that the mass resolution is not critical for m_H=200 GeV. In particular it is much larger than the natural width in all cases, and a SM Higgs signal could only be separated from a MSSM Higgs signal for larger Higgs masses, as discussed below.

We now consider, as an example, the case where m_H=300 GeV, for which the SM natural width is large, Γ_H^{SM} = 8.3 GeV, whereas in the MSSM the width varies from 0.26 GeV for $tan\beta$=3 up to 0.7 GeV for $tan\beta$=10. Table 6 summarizes the mass resolutions and the acceptances in the mass bin (with and without Z-mass constraint) in the 4-muon mode. The mass resolution obtained with full simulation for the 4-electron mode is 2.9 GeV (resp. 3.1 GeV) at low (resp. high) luminosity.

$H \rightarrow ZZ \rightarrow 4\ \mu$	Stand-alone		Combined	
m_H = 300 GeV	σ_m (GeV)	# in $\pm 2\sigma_m$ (%)	σ_m (GeV)	# in $\pm 2\sigma_m$ (%)
Air-Air B=1.00	3.5	91	2.9	93
Air-Air B=0.85	4.0	91	3.2	93
With Z-mass const.	4.7	81	-	-
Air-Air B=0.70	4.6	91	3.6	93
Air-Fe B=0.85	5.6	77	4.0	91
With Z-mass const.	5.1	81	-	-
Air-Fe staged	5.6	74	4.0	90
With Z-mass const.	5.2	79	-	-

Table 6: *For $H \rightarrow ZZ \rightarrow 4\ \mu$ decays with m_H = 300 GeV, and for various configurations of the muon system, mass resolutions (after subtraction of the SM Higgs boson width), and acceptances in mass bin (with and without Z-mass constraint). The results are shown for both the stand-alone (left) and combined (right) measurements.*

The Z-mass constraint is shown to improve slightly the Higgs mass resolution and the acceptance in the mass bin, only for the systems with iron-core end-caps. It however deteriorates the Higgs mass resolution for full air-core systems.

Fig. 14 shows for the full-air core system and for the two systems with iron-core

end-caps, the expected 4-muon mass spectrum for stand-alone measurements, both for a SM Higgs of 8.3 GeV width and for a MSSM Higgs, of negligible width with respect to the detector mass resolution. A good mass resolution will clearly be a useful tool to distinguish between different models by either measuring the Higgs boson width or setting an upper limit on its width. It should be reiterated here that the full statistics of the electron and muon channels will be necessary for an optimal sensitivity to a possible signal, since the MSSM $H \rightarrow ZZ \rightarrow 4l$ rates are strongly suppressed with respect to the SM. In fact, the rate measurement is likely to be the most sensitive method for establishing the nature of the signal.

4 MSSM $A/H \rightarrow \mu^+\mu^-$, $m_{A/H} = 300$ GeV

This channel is of interest in the MSSM , and has negligible rate in the electron mode. The expected rates in the $\tau\tau$ mode are however much larger by a factor $(m_\tau/m_\mu)^2$, but the better mass resolution expected in the muon channel may provide some sensitivity to $tan\beta$. A value $m_{A/H} = 300$ GeV, typical of the accessible region for this channel in the MSSM, has been studied. The natural width varies from a few GeV to $\simeq 20$ GeV as a function of $tan\beta$ [8].
The di-muon channel suffers from large backgrounds from Drell-Yan and $t\bar{t}$, which is of course an incentive for good mass resolution.
A simple event selection requires 2 muons with $p_T > 20$ GeV, and $|\eta| < 2.5$, with $p_T^{\mu\mu} > 20$ GeV, as described in [8].

Table 7 summarizes the expected mass resolutions and the acceptances in the mass bin, for various muon systems configurations, and for stand-alone and combined measurements.

$A/H \rightarrow \mu^+\mu^-$	Stand-alone		Combined	
$m_H = 300$ GeV	σ_m (GeV)	# in $\pm 2\sigma_m$ (%)	σ_m (GeV)	# in $\pm 2\sigma_m$ (%)
Air-Air B=1.00	4.6	92	idem	idem
Air-Air B=0.85	5.3	91	idem	idem
Air-Air B=0.70	6.2	89	idem	idem
Air-Fe B=0.85	6.0	74	6.0	87
Loss in signif.	31%		11%	
Air-Fe staged	6.4	67	6.2	86
Loss in signif.	49%		14%	

Table 7: *For $A/H \rightarrow \mu^+\mu^-$ decays with $m_H = 300$ GeV, and for various configurations of the muon system, mass resolutions (after subtraction of the Higgs boson width), fraction of non-Gaussian tails and losses in significance with respect to the full air-core system with B=0.85. The results are shown for both the stand-alone (left) and combined (right) measurements.*

It can be seen that both iron-core end-cap systems would provide a strongly

degraded overall acceptance for the signal, because of large tails in the mass distribution. As shown in Table 7 and also in Fig. 15, the tracker does not help to improve the mass resolution at these high momenta, but it does help in recovering almost completely the non-Gaussian tails induced by muons measured in the iron-core end-caps, thus limiting the loss in significance to 10-15% with respect to the stand-alone full air-core case.

In the case of the full air-core system, the measurement of the $A/H \rightarrow \mu^+\mu^-$ experimental signal width would provide sensitivity to values of $tan\ \beta \geq 35$ ($\Gamma_{A/H} \simeq$ 8 GeV). This sensitivity would be limited to values of $tan\ \beta \geq 40$ ($\Gamma_{A/H} \simeq$ 10 GeV) for descoped systems.

5 Heavy $Z' \rightarrow \mu^+\mu^-$, $m_{Z'} = 3$ TeV

New heavy neutral gauge bosons are expected to decay into e^+e^-, $\mu^+\mu^-$ and jet-jet pairs. Previous studies in ATLAS [9, 10] have shown that :
• the e^+e^- channel will be the best to discover a possible signal and measure its width.
• The $\mu^+\mu^-$ channel will be the best to measure the forward/backward asymmetry and thus provide important constraints on the model.
• The dijet channel, although suffering from very large QCD backgrounds, will also be observable in many cases, and thus will provide additional constraints on the model.

A heavy Z' with $m_{Z'} = 3$ TeV has been studied in this note. In the Natural Extension of the Standard Model, the neutral gauge boson width scales with its mass, $\sigma_m \simeq 35$ GeV for $m_{Z'} = 3$ TeV. To better evaluate the detector contribution to the mass resolution, the effect of this natural width has been subtracted event by event for the studies presented here.
The extraction of the signal is straightforward, since the background (mainly Drell-Yan) is very small at these high masses.

Fig. 16 shows the expected Z' mass distributions for various muon systems configurations, which are summarized in Table 8, as well as the resolutions expected in the electron and di-jet mode.
About 70% of the Z'-decays have both final-state muons measured in the barrel air-core magnet. The mass resolutions scale with the field, as expected, but they clearly cannot compete with the ones obtained in the other decay modes.

This is also important to recall, that it has been shown a long time ago that the lepton (muon or electron) momentum resolution has a negligible effect on the asymmetry measurement accuracy [11], since only the sign of the charge is important for such measurements. Similar conclusions, although less strongs, apply to the case of heavy charge gauge bosons W'.

σ_m (GeV)	$\mu\mu$	ee	jet-jet
Air-Air B=1.00	180	21	66
Air-Air B=0.85	200		
Air-Air B=0.70	240		
Air-Fe B=0.85	220		
Air-Fe staged	260		

Table 8: *For $m_{Z'} = 3$ TeV, mass resolutions (after subtraction of the natural Z' width) for various muon systems configurations.*

6 CONCLUSIONS

The potential losses in physics performance of the ATLAS detector, for the various options concerning the staging and descoping of the muon system, have been evaluated and summarized in this note, using particle-level simulations and detailed parametrizations of the expected resolutions. The list of physics processes studied here, although representative of a large range of channels with muons in the final state, cannot be exhaustive and thus may not fully cover the physics potential of ATLAS.

For all the channels studied here, a clear degradation of performance is observed for the "stand-alone" muon measurements in most staging and descoping scenarios. Most of this degradation of performance disappears, however, when the full potential of the ATLAS detector (inner detector) and of the physics itself (electron final states) is used.

In particular, for the most delicate case in terms of overall rate and signal-to-background ratio, i.e. the search for $H \rightarrow ZZ^* \rightarrow 4$ lepton decays and for integrated luminosities up to 10^5 pb^{-1}, a signal above 3σ significance cannot be observed over the full mass range of interest in the 4-muon mode alone, whether using "stand-alone" or combined measurements. The full statistics, electrons and muons, have to be combined, and, in addition, the inner detector information is not only important to improve the mass resolution of the 4-muon channel, but also essential in bringing the reducible backgrounds safely below the irreducible continuum background.

References

[1] C. Guyot, private communication, and ATLAS internal note, MUON-No-065, 1995.

[2] A. Henriques et al., TILECAL-note 068, 1995.

[3] O. Linossier and L. Poggioli, ATLAS internal note, PHYS-No-075, 1995.

[4] A. Nisati et al., Aachen Workshop, Vol. II, 1990.

[5] R. St-Denis, ATLAS internal note, PHYS-No-011, 1992.

[6] ATLAS staging and descoping document, CERN/LHCC/95-68, 1995.

[7] E. Richter-Was et al., ATLAS internal note, PHYS-No-048, 1995.

[8] E. Richter-Was et al., ATLAS internal note, PHYS-No-074, 1995.

[9] A. Henriques and L. Poggioli, ATLAS internal note, PHYS-No-010, 1992.

[10] M.-C. Cousinou, ATLAS internal note, PHYS-No-059, 1994.

[11] B. Dolgoshein et al., RD6 Status Report, CERN/DRDC/91-47, 1991.

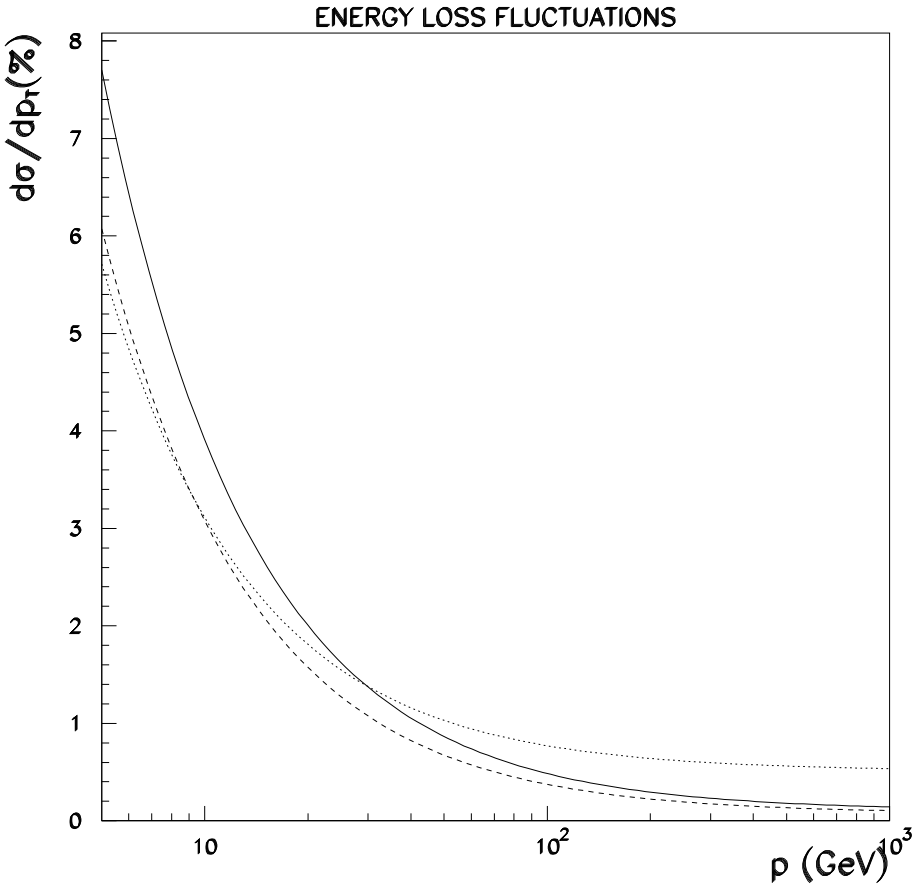

Figure 4: *Contribution to the muon momentum resolution of the energy loss fluctuations in the calorimeter versus the muon momentum. The solid curve corresponds to a realistic estimate using the tile calorimeter measurement in the ATLAS setup where both the electromagnetic calorimeter and the tile support are assumed to provide no information (about 30% of the total interaction length). The dashed curve corresponds to the ideal case where the full material traversed by the muon would be instrumented. The dotted curve represents the estimated effective r.m.s. of the energy loss fluctuations.*

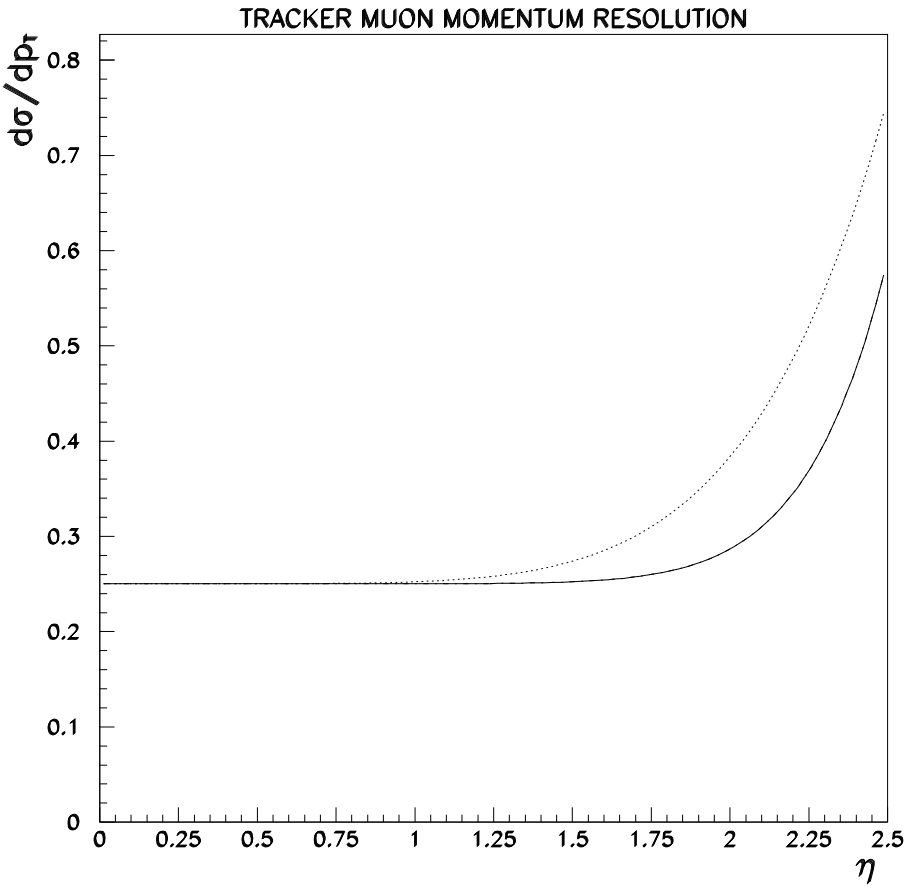

Figure 5: *Parametrized inner detector p_T-resolution, for $p_T = 500$ GeV, as a function of η, for the Morges layout (full line) and the shorter cavity with a shorter coil (dotted line).*

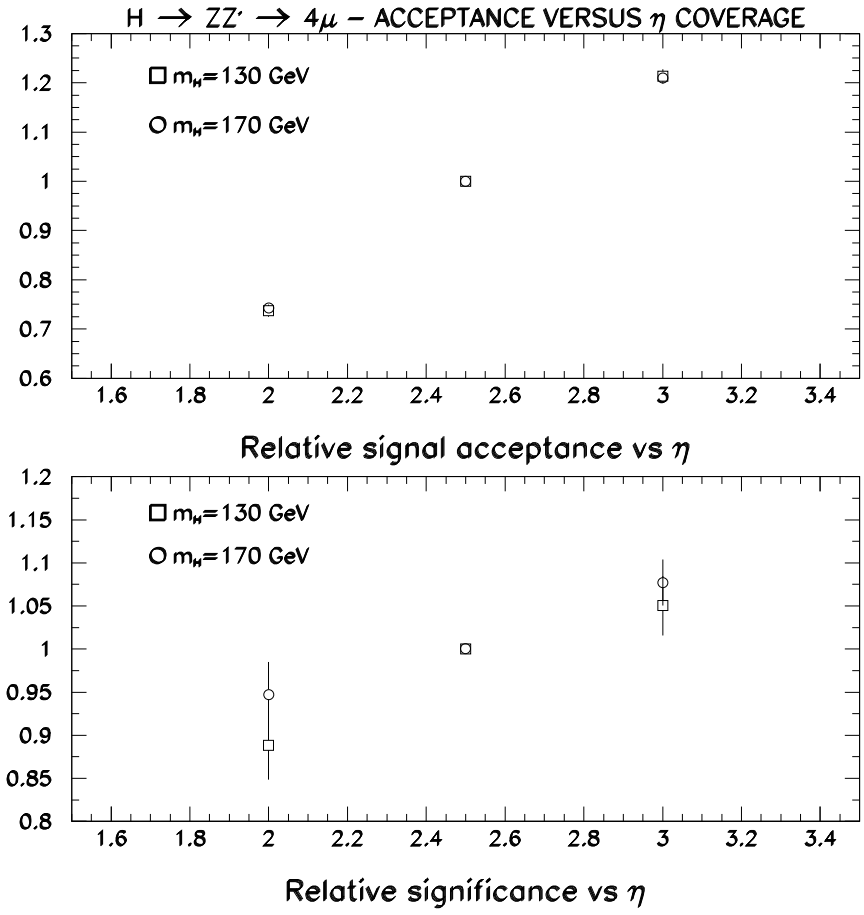

Figure 6: *For $H \rightarrow ZZ^* \rightarrow 4\mu$ decays, relative signal acceptance (top) and statistical significance (bottom) versus maximum rapidity coverage, normalized to $\eta = 2.5$. The significances are estimated in the optimistic case where the only remaining background is the irreducible ZZ^*/γ^* continuum. The effects are somewhat larger for lower Higgs masses, since the decay products are less central.*

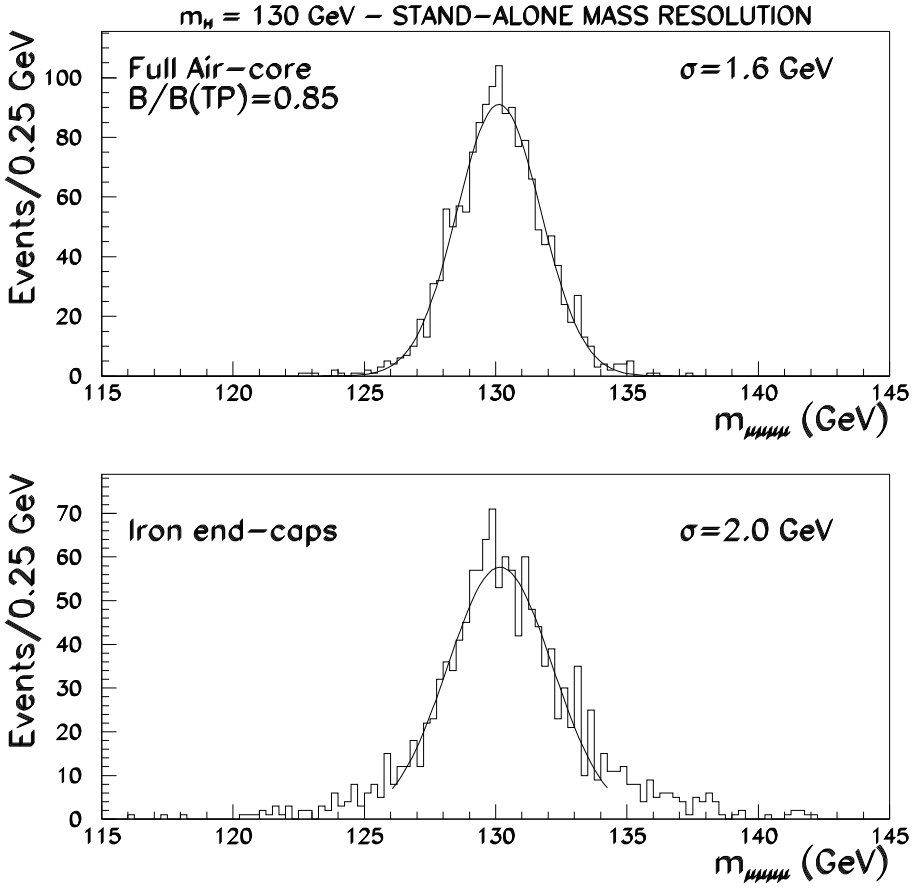

Figure 7: *For $H \rightarrow ZZ^* \rightarrow 4\mu$ decays with $m_H = 130$ GeV, stand-alone mass resolution for the full air-core system (top), and for the system with 4.6 m long iron-core end-caps (bottom).*

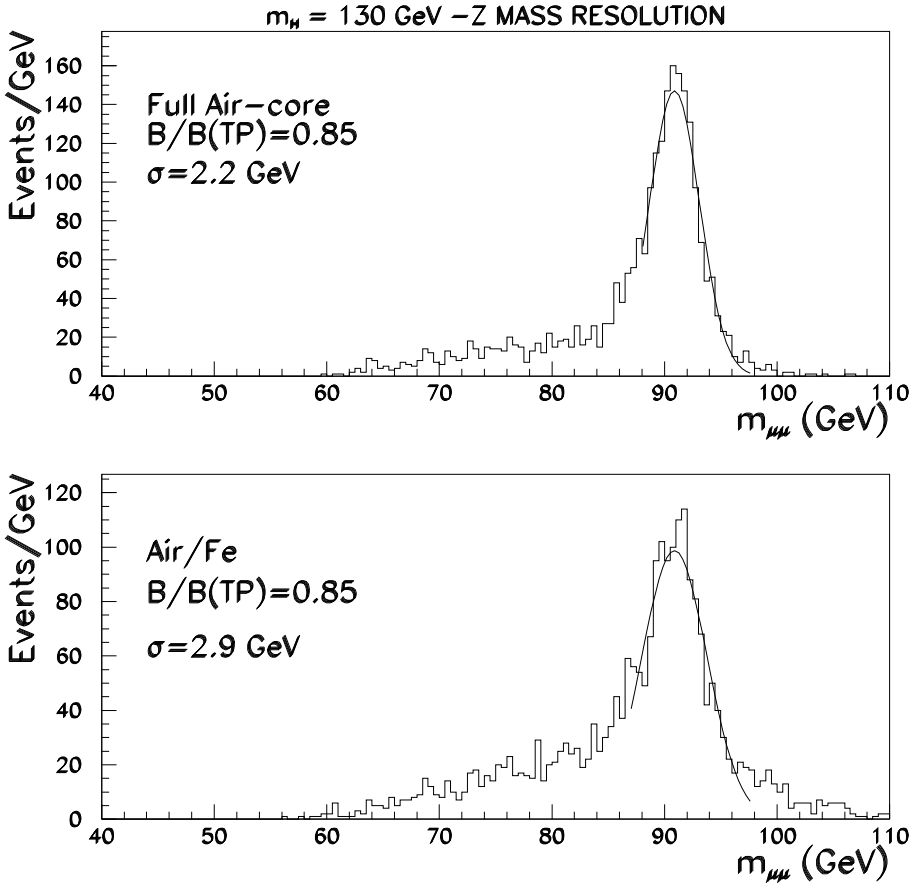

Figure 8: *For $H \rightarrow ZZ^* \rightarrow 4\mu$ decays with m_H= 130 GeV, stand-alone mass resolution for $Z \rightarrow \mu^+\mu^-$ for the full air-core system (top), and for the system with 4.6 m long iron-core end-caps (bottom).*

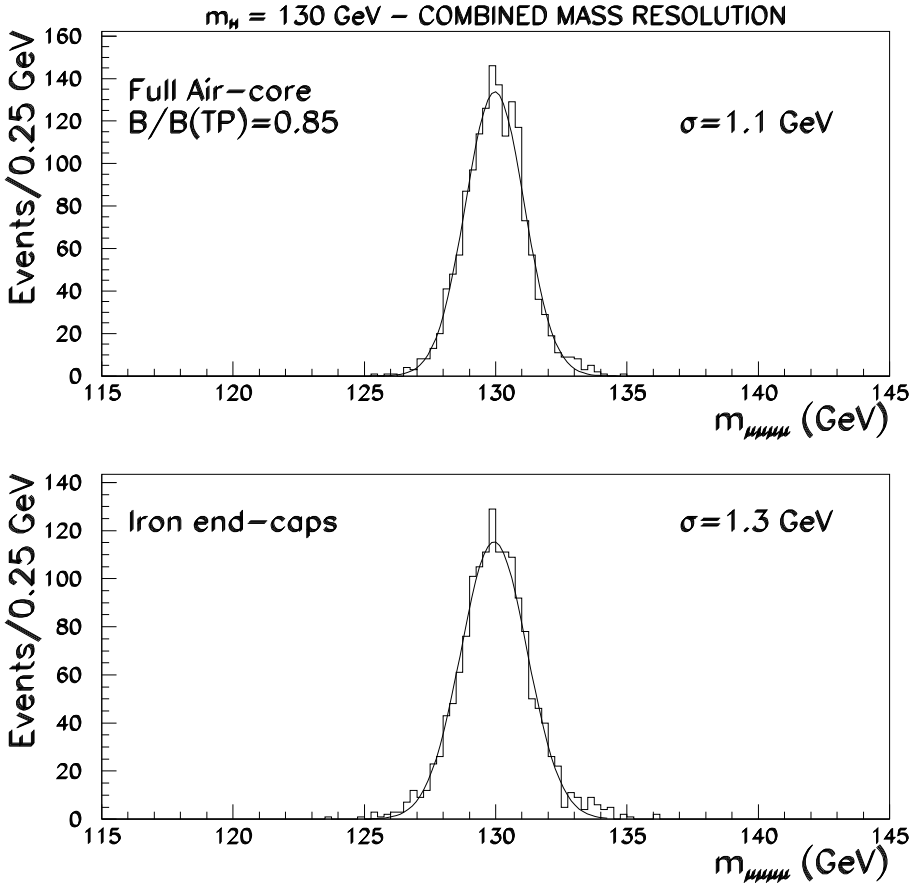

Figure 9: *For $H \rightarrow ZZ^* \rightarrow 4\mu$ decays with $m_H = 130$ GeV, combined mass resolution for the full air-core system (top), and for the system with 4.6 m long iron-core end-caps (bottom).*

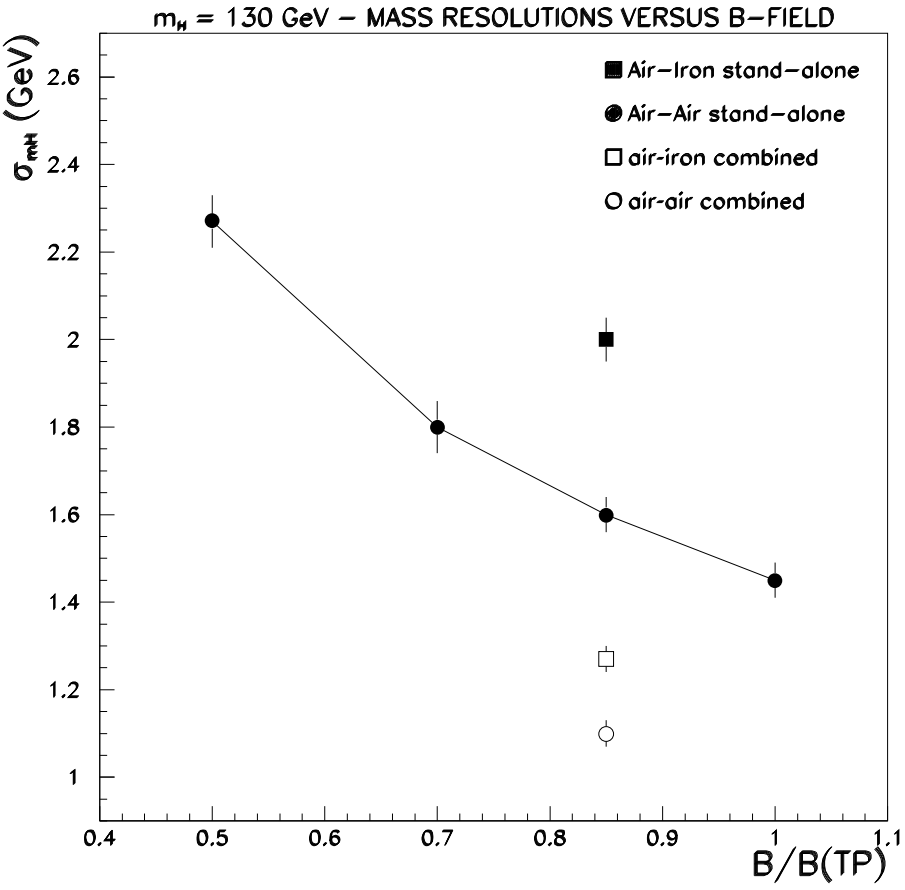

Figure 10: *For $H \rightarrow ZZ^* \rightarrow 4\mu$ decays with $m_H = 130$ GeV, expected mass resolutions for various toroid field values and magnet systems.*

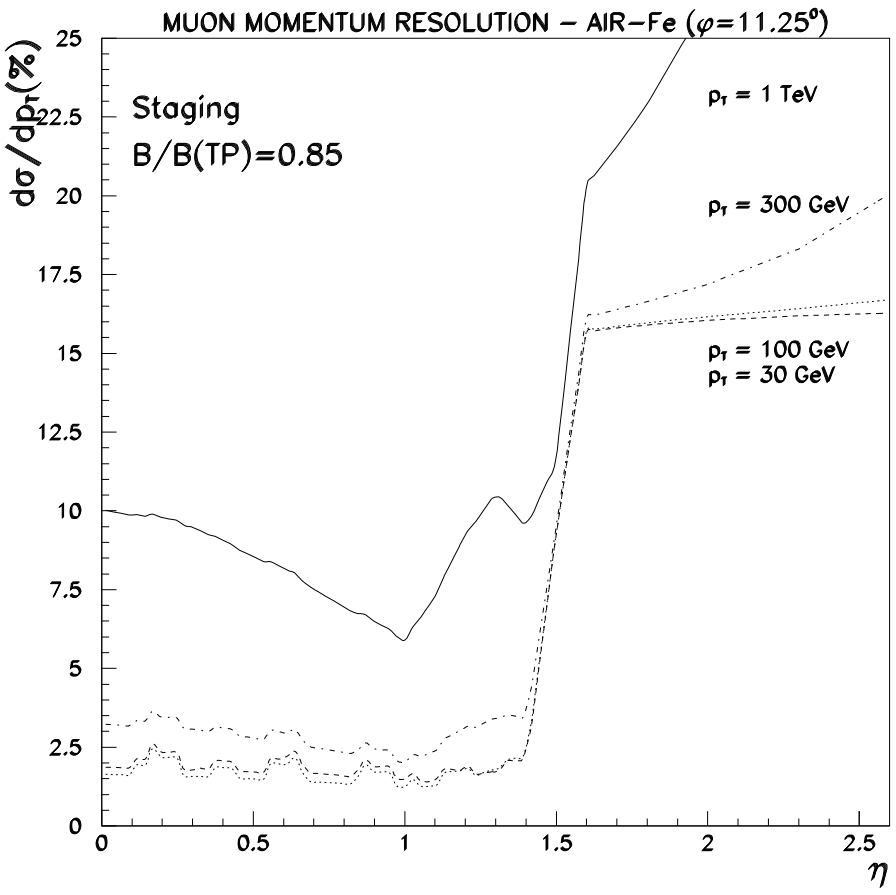

Figure 11: *Expected p_T-resolutions versus η for the air-core with 2 m long iron-core end-caps system, for $\phi = 11.25^0$ with respect to a coil.*

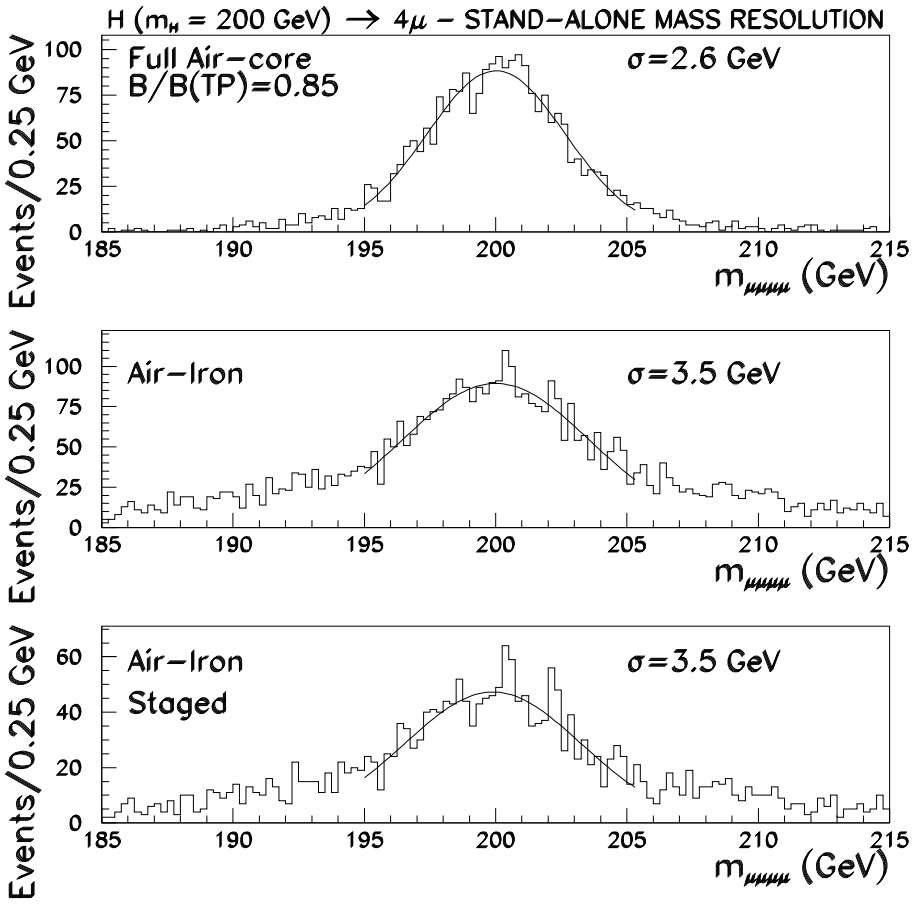

Figure 12: *For $H \rightarrow ZZ \rightarrow 4\mu$ decays with $m_H = 200$ GeV, stand-alone mass resolution for the full air-core system (top), for a system with 4.6 m long iron-core end-caps (middle), and for a system with staged 2 m long iron-core end-caps (bottom).*

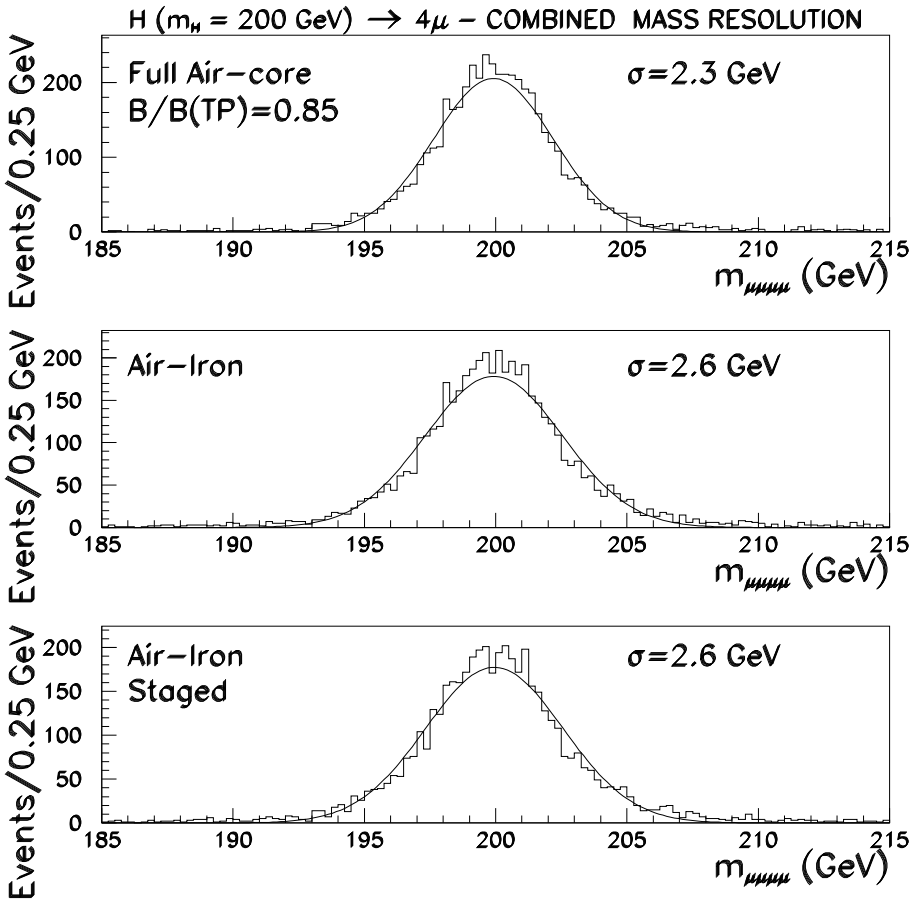

Figure 13: *For For $H \rightarrow ZZ \rightarrow 4\mu$ decays with $m_H = 200$ GeV, combined mass resolution for the full air-core system (top), for a system with 4.6 m long iron-core end-caps (middle), and for a system with staged 2 m long iron-core end-caps (bottom).*

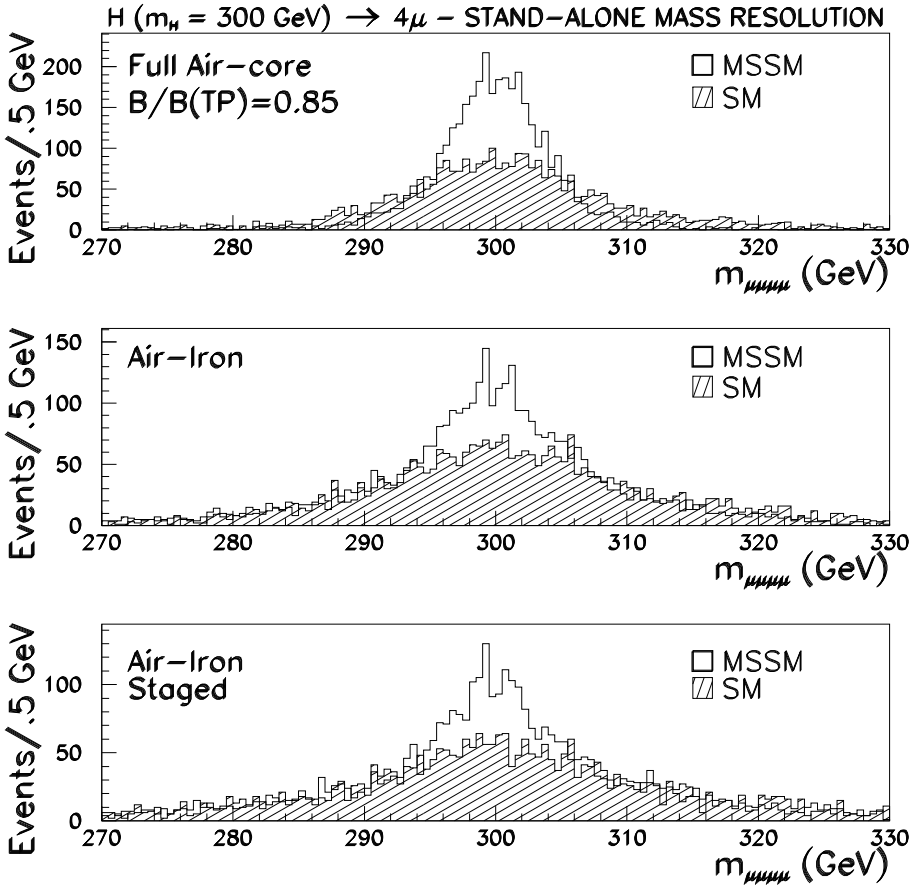

Figure 14: *For $H \rightarrow ZZ \rightarrow 4\mu$ decays with $m_H = 300$ GeV, stand-alone mass resolution for the full air-core system (top), for a system with 4.6 m long iron-core end-caps (middle), and for a system with staged 2 m long iron-core end-caps (bottom). For each case, the 4-muon mass spectrum is shown, both for a Standard Model Higgs (hatched histogram) and a MSSM Higgs with negligible Γ_H (white histogram). Both histograms have the same number of entries.*

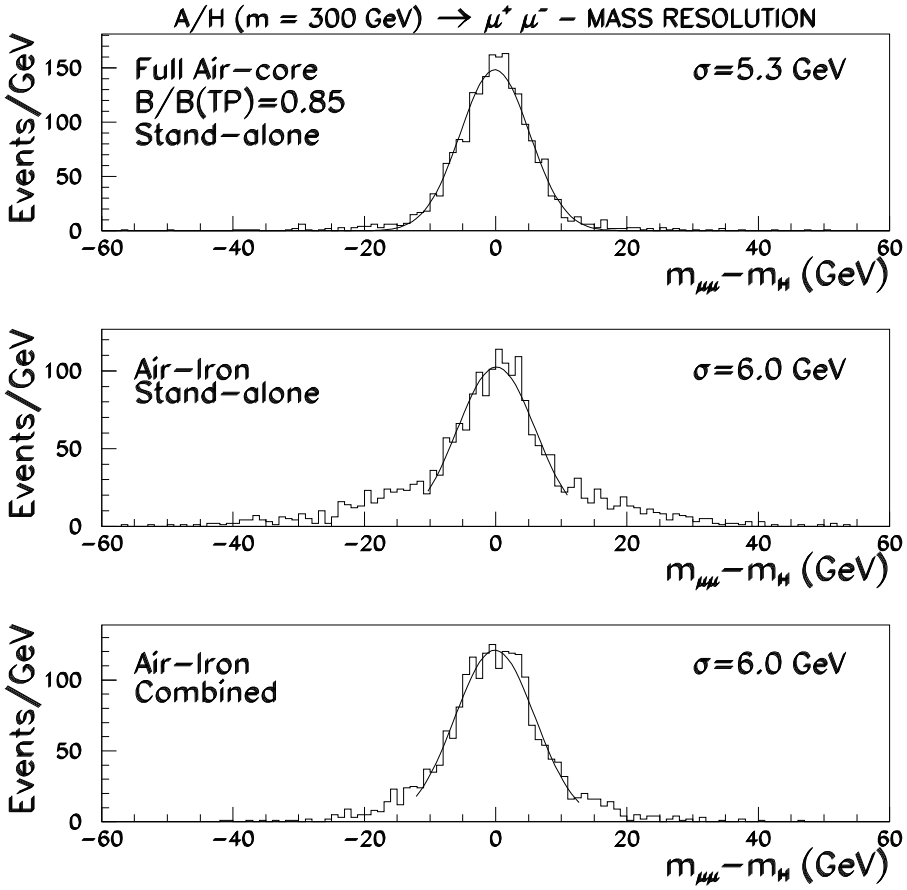

Figure 15: *For $A/H \rightarrow \mu^+\mu^-$ decays with m_H=300 GeV, expected mass resolutions (after subtraction of the Higgs boson width), in the case of the stand-alone measurement for the full air-core system (top), the stand-alone measurement for a system with 4.6 m long iron-core end-caps (middle), and the combined measurement for a system with 4.6 m long iron-core end-caps (bottom).*

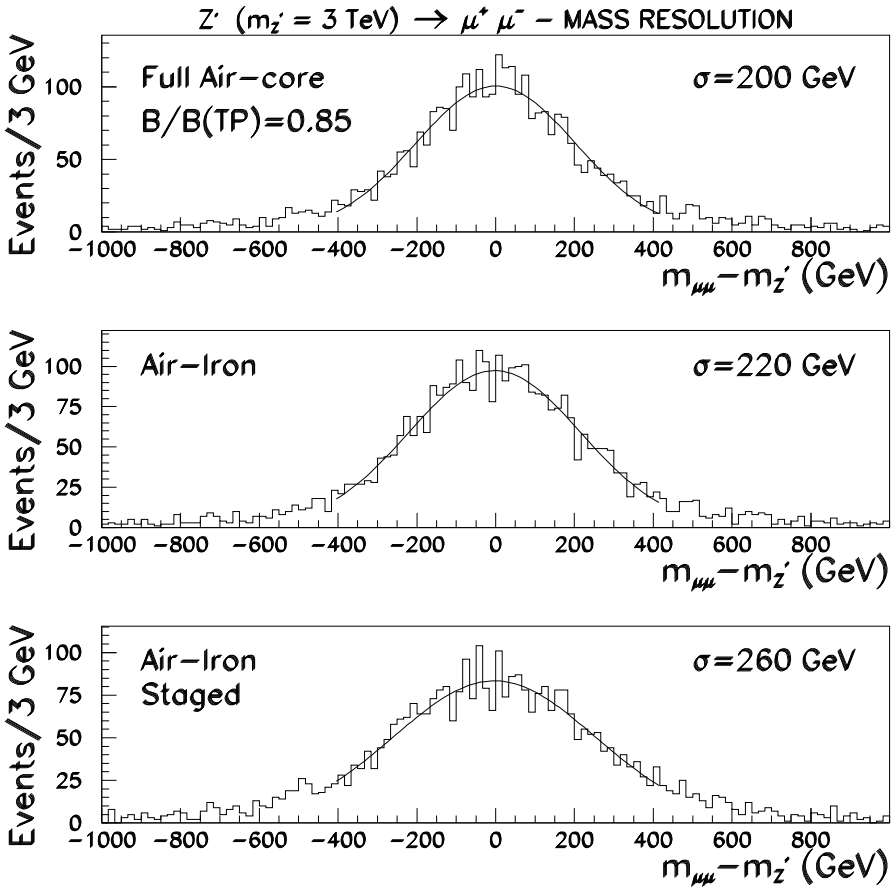

Figure 16: *For $Z' \to \mu^+\mu^-$ decays with $m_{Z'} = 3$ TeV, expected stand-alone mass resolution (after subtraction of the natural width of the Z') for the full air-core system (top), for a system with 4.6 m long iron-core end-caps (middle), and for a system with staged 2 m long iron-core end-caps (bottom).*